Access the most recent version at http://jeb.biologists.org/lookup/doi/10.1242/jeb.156836

Humeral loads during swimming and walking in turtles: implications for morphological change during aquatic reinvasions

Vanessa K Hilliard Young[1], Charlotte E. Wienands, Brittany P. Wilburn, Richard W. Blob

Department of Biological Sciences, Clemson University, Clemson, SC 29634

[1]Corresponding Author:
Vanessa K Hilliard Young
Department of Biological Sciences
Clemson University
132 Long Hall
Clemson, SC 29634
vkhilli@clemson.edu

Key words: bone strain, *Pseudemys concinna*, evolution, locomotion

ABSTRACT

During evolutionary reinvasions of water by terrestrial vertebrates, ancestrally tubular limb bones often flatten to form flippers. Differences in skeletal loading between land and water might have facilitated such changes. In turtles, femoral shear strains are significantly lower during swimming than during walking, potentially allowing a release from loads favoring tubular shafts. However, flipper-like morphology in specialized tetrapod swimmers is most accentuated in the forelimbs. To test if the forelimbs of turtles also experience reduced torsional loading in water, we compared strains on the humerus of river cooters (*Pseudemys concinna*) between swimming and terrestrial walking. Humeral shear strains are also lower during swimming compared to terrestrial walking; however, this appears to relate to reduction in overall strain magnitudes, rather than a specific reduction in twisting. These results indicate that shear strains show similar reductions between swimming and walking for forelimb and hindlimb, but these reductions are produced through different mechanisms.

INTRODUCTION

Habitat transitions have driven evolutionary change in many vertebrate lineages, often leading to specialization for novel environments and radiations of species (Ashley-Ross et al., 2013; Blob et al., 2016). Several ancestrally terrestrial tetrapod lineages (e.g. cetaceans, mosasaurs, manatees, sea turtles) have evolved fully aquatic lifestyles characterized by changes in body and limb shape (Zimmer, 1999; Caldwell, 2002; Lindgren et al., 2011). For example, terrestrial tetrapods have limb bones that are tubular in cross-section, shapes that help to optimize resistance to twisting (Buckwalter et al., 1995; Vogel, 2013; Blob et al., 2014); in contrast, many tetrapods that become secondarily specialized for aquatic environments exhibit flattening of the limbs (Zimmer, 1999; Renous et al., 2008). Such shapes are advantageous for producing both drag- and lift-based thrust during swimming once they are established (Walker, 2002), but the factors that promoted evolutionary transitions from tubular to flattened limbs are less clear.

Because the shapes of bones are known to respond to changes in loading environment over both ontogenetic and evolutionary time scales (Lanyon et al., 1982; Bertram and Biewener, 1990), and because buoyancy conveyed by water should reduce the loads placed on the skeleton to support the body (Zug, 1971), we previously proposed that changes in limb bone loading between land and water might have facilitated the evolution of flattened limbs in secondarily aquatic tetrapods (Young and Blob, 2015). Specifically, because torsional loading is high in the limb bones of many tetrapods (Biewener and Dial, 1995; Blob and

Biewener, 1999; Butcher et al., 2008; Sheffield et al., 2011), and tubular shapes are well suited to resist torsion (Vogel, 2013), we proposed that a reduction of torsion in particular could have released the limbs from an environment favoring tubular bones and, thereby, facilitated the evolution of flattened shapes (Young and Blob, 2015). To test this proposal, we compared *in vivo* bone strains between terrestrial walking and swimming for the femur of semi-aquatic slider turtles, *Trachemys scripta* (Young and Blob, 2015). Turtles are advantageous models for these comparisons because the fusion of the vertebrae to the shell means that propulsion is generated exclusively by the limbs, and comparisons between environments are not confounded by shifts between axial and appendicular propulsion (Gillis and Blob, 2001). Our choice of a semi-aquatic species as a model reflected its use of rowing limb movements, which were also likely used by species in the initial stages of aquatic reinvasions (Fish, 1996). Moreover, our focus on the femur reflected the dominant propulsive role of the hindlimb in semi-aquatic turtles (Blob et al., 2008). Our results showed that torsional shear strains on turtle femora did, in fact, decrease much more than bending strains between terrestrial walking and swimming (Young and Blob, 2015). These results were due partly to an overall decrease in load magnitudes in water. However, they also resulted from a substantial change in loading regime, in which principal strains became reoriented to align much more closely with the long axis of the femur during swimming (6.1°) than during walking (19.8°). These patterns indicated sharply reduced twisting of the femur about its long axis during swimming, a conclusion that was verified by subsequent XROMM observations of femoral kinematics in turtles (Mayerl et al., 2016).

Although strain data from turtle femora indicate that reduced torsional loads during aquatic locomotion could have generated a mechanical environment favorable for the evolution of non-tubular limb bones, the restriction of these data to the femur is problematic. In most lineages of tetrapods that became secondarily specialized for aquatic locomotion, including sea turtles, the forelimbs come to dominate appendicular-based propulsion (Wyneken, 1997; Blob et al., 2016). Thus, if changes in loading are to provide a plausible mechanism that could have contributed to the evolution of flattened limbs during aquatic reinvasions, then a reduction in torsion during swimming should be found in the humerus as well as the femur. However, no loading data are available for the forelimbs of any turtle, or any swimming tetrapod. To test whether loading patterns differ between terrestrial walking and swimming for the forelimb, we collected *in vivo* humeral strain data from semi-aquatic river cooter turtles, *Pseudemys concinna* (LeConte 1830), a species that is closely related and ecologically similar to *T. scripta* (Ernst and Lovich, 2009), but which reaches larger body

sizes that facilitate strain gauge implantation onto the humerus. If the humerus does not show reduced torsion during swimming in turtles, then the plausibility of limb bone flattening having been facilitated by environmental changes in loading regime would be called into question.

MATERIALS AND METHODS

Animals

Six adult *P. concinna* (3 females, 3 males; carapace length 28.15 ± 2.46 cm; mass 2.65 ± 0.61 kg) were collected from Lake Hartwell, Pickens County, SC, USA (August 2013 and August 2014, South Carolina Department of Natural Resources Permits 43-2013, 29-2014). Housing and husbandry followed published standards (Butcher et al., 2008).

Surgical procedures

All procedures were approved by the Clemson University IACUC (AUP 2012-056, 2016-011). To induce analgesia and anesthesia, turtles were injected (left forelimb muscles) with doses of 1 mg kg^{-1} butorphenol, 100 mg kg^{-1} ketamine, and 1 mg kg^{-1} xylazine (supplemented as needed). Upon achieving anesthesia, a medial incision was made along the proximal aspect of the right forelimb. Muscles surrounding the humerus were separated and retracted to expose gauge attachment sites. A window of periosteum was removed, and the exposed bone cortex was swabbed clean with ether. Single element and rosette strain gauges (FLG-1-11 and FRA-1-11, respectively; Tokyo Sokki Kenkyujo, Japan) were attached using self-catalyzing adhesive (Duro® Super Glue; Henkel Corporation, Avon, OH, USA). In our largest individual, we implanted a rosette gauge on both the anterior and posterior surface of the humerus. In other large individuals, we attached a rosette gauge to either the anterior or ventral surface, and single-element gauges to two other surfaces (anterior, ventral, or posterior). For our smallest individuals, in which rosette gauges could not be implanted due to size limitations, three single-element gauges were attached in anterior, ventral, and posterior positions. Once gauges were in place, lead wires were threaded through a second, proximal forelimb incision. Incisions were sutured closed, and wires were soldered to a microconnector and sealed with epoxy. Connectors were secured to the forelimb with self-adhesive bandage (Vetrap®; 3M Animal Care Products, USA), with care taken to avoid restricting limb movement.

In vivo strain data collection and data analysis

Following 24 hours of recovery, *in vivo* strain data were collected during steady speed swimming in a flow tank and walking on a motorized treadmill (model DC5; Jog A Dog®; Ottowa Lake, MI, USA). Strain signals were conducted from the gauges to Vishay conditioning bridge amplifiers (model 2120B; Measurements Group, Raleigh, NC, USA) by a shielded cable. To prevent signal disruption by water, the connection between this cable and the connector attached to the turtle was sealed with Plumber's Epoxy Putty (ACE Hardware Corporation, USA). Raw voltages from strain gauges were sampled through an A/D converter (model PCI-6031E; National Instruments) at 5000 Hz. These data were saved to computer using data acquisition software (LabVIEW v. 6.1; National Instruments) and calibrated to microstrain (με).

Trials were conducted at the maximal speed at which an individual could maintain its position in the flow tank or on the treadmill (0.200-0.495 m s^{-1} in flowtank; 0.103-0.139 m s^{-1} on treadmill). Although these speeds are not strictly dynamically equivalent, they provide comparable levels of exertion that are useful for understanding selection pressures acting on skeletal design. High-speed videos of each trial were recorded from lateral and ventral (swimming) or dorsal (walking) views (100 Hz; Phantom V5.1, Vision Research Inc., Wayne, NJ, USA). Videos were synchronized with strain recordings using a light box that emitted a visible flash in the video that corresponded with a 1.5V pulse in the strain recording. Strain recordings were zeroed by selecting samples of 100 values from each trial during intervals of limited motion (swimming) or resting with the shell on the treadmill (walking). Upon completion of trials, turtles were euthanized via intraperitoneal injection (Euthasol® pentobarbital sodium solution; Delmarva Laboratories Inc., Midlothian, VA, USA; 200 mg kg^{-1}).

Due to gauge failure at some sites, particularly during aquatic trials, strain data were only collected from a subset of the locations at which gauges were initially implanted. As a result, longitudinal strain data were collected from the posterior surface of the humerus for three individuals, the ventral surface for three individuals, and the anterior surface for one individual. Swimming principal strains were collected from three individuals, and terrestrial walking principal strains were collected from two individuals (Tables 1 and 2). Peak strain magnitudes were determined from each functioning gauge location for each stroke (swimming) and step (walking) of the right forelimb, following previously published methods (Blob and Biewener, 1999). Walking and swimming strains were compared within each

individual for each gauge location using Mann-Whitney *U*-tests. Statistical analyses were conducted in SAS® (v. 9.3, SAS Institute Inc. 2010, Cary, NC, USA).

RESULTS AND DISCUSSION

During swimming, longitudinal strains generally maintained the same orientation (i.e. tensile or compressive) during both thrust (retraction) and recovery (protraction) phases of the limb cycle for four out of seven comparisons (Table 1). Thus, the humerus showed reversals in its direction of bending between protraction and retraction more frequently than the femur (Young and Blob, 2015). Single peaks were typically observed during retraction in swimming, whereas strains were more variable during protraction (Fig. 1), resembling patterns observed in the femur (Butcher et al., 2008; Young and Blob, 2015). In contrast to the femur (Young and Blob, 2015), absolute magnitudes of peak humeral strain during swimming (longitudinal, principal, and shear) were not uniformly greater during thrust than during recovery (Table 1). These differences between humeral and femoral loading may reflect differences in the size of the paddle formed by the foot in each limb. In both limbs, the foot is rotated perpendicular to oncoming flow during retraction (Pace et al., 2001; Blob et al., 2008), maximizing surface area of the foot against the surrounding medium to produce drag-based thrust. During recovery phase (protraction), the foot is rotated parallel to oncoming flow, reducing drag and minimizing interference to forward motion of the body. Such drag reduction is expected to minimize the environmental forces acting on the limb, resulting in lower strains during recovery (Young and Blob, 2015). However, the surface area of the forefoot paddle is much smaller than the surface area of the hindfoot paddle in cooters and sliders (Young et al., 2017), which may lead to greater similarity in the environmental forces applied to the limb between thrust and recovery phases for the forelimb. Moreover, orientation of peak principal tensile strain to the long axis of the humerus (φ_T) was typically near 45° during both thrust and recovery, indicating the significance of twisting as a mechanism through which loads are applied to the forelimb (Table 1). These orientations are a further departure from the patterns observed in the femur, in which (φ_T) was closer to 0° during both thrust and recovery.

In comparisons between swimming and walking, the orientation of longitudinal strains on the humerus was typically consistent between environments (4 of 6 comparisons: Table 2). Peak strain magnitudes also were consistently significantly lower during the thrust phase of swimming than during the stance phase of walking (Table 2, Fig. 1). For

longitudinal strains during retraction, peak magnitudes during swimming were approximately 11% of peak magnitudes during walking. For shear, however, peak swimming strain magnitudes were roughly 40% of walking strains (Table 2, Fig. 1). Though this is a considerable reduction in loads between locomotor environments, it is less of a reduction in shear between environments than was found for the femur, in which shear strains during swimming were only 10% of those during walking (Young and Blob, 2015). In the femur, shear strain reduction during swimming is driven by both an overall reduction in strain magnitudes conveyed by buoyancy in water, and through a reorientation of loading that reduces the high levels of twisting observed in walking to lower levels during swimming (Young and Blob, 2015; Mayerl et al., 2016). In contrast, the reduction of humeral shear strains during swimming appears to result essentially solely from the overall reduction of strain magnitudes in water compared to land (Table 2). Values of φ_T for the humerus (Table 2) are substantially greater than 0° during both terrestrial walking and swimming, indicating that twisting is likely applied to the humerus in both environments. Therefore, though both shear and torsional loading on the humerus are reduced during swimming compared to walking, this reduction does not appear to result from the substantial reorientation of applied loads that occurs in the femur.

The different mechanisms that reduce aquatic shear strains in the humerus versus the femur of turtles may relate to structural differences between the forelimb and hindlimb, and the kinematic constraints that these impose. The extent of forelimb protraction in turtles is unusually high for tetrapods with sprawling postures (Walker, 1971; Pace et al., 2001; Schmidt et al., 2016). Such protraction may be facilitated by humeral morphology, particularly its arched shaft and the anatomical torsion of the distal humerus relative to the head (Ogushi, 1911). However, humeral retraction in turtles is generally limited (Rivera and Blob, 2010; Schmidt et al., 2016), likely due to restrictions imposed by the anterior edge of the bridge between the carapace and plastron (Walker, 1971; Zug, 1971). As a potential consequence, in tortoises walking on land, the majority of forelimb range of motion (64%) is derived from long axis rotation, combined with elbow extension (Schmidt et al., 2016). Given the large potential impact of axial rotation on the range of forelimb motion, a reduction of humeral twisting in water might impose substantial locomotor restrictions on turtles. Therefore, long-axis rotation of the humerus may be necessary in both aquatic and terrestrial habitats in order to achieve adequate range of motion for forward propulsion, and could explain why strain orientations near 45° are observed in both habitats. Such locomotor

restrictions of the humerus stand in contrast to the limited impact that reduced femoral twisting appears to have on hindlimb movements (Mayerl et al., 2016), as the hindlimbs do not experience the same degree of shell obstruction and, therefore, do not need to maintain long-axis rotation to sustain limb excursion and generate thrust in aquatic environments.

Strain patterns of the long bones of the limb indicate reduced shear during swimming compared to terrestrial walking in both the forelimb and the hindlimb (Young and Blob, 2015). Despite showing similar patterns of shear reduction, changes in loading between land and water may occur through different mechanisms in the humerus and femur that relate to structural and functional differences between the forelimb and hindlimb in turtles. Nonetheless, the distinctive changes in long bone morphology that characterize most reinvasions of aquatic habitats by tetrapods may likely have been facilitated by release from the demands imposed by body support and torsional loading, allowing greater opportunity for the evolution of novel limb bone shapes.

ACKNOWLEDGEMENTS

We thank C. Mayerl, K. Diamond, J. Pruett, K. Vest, and M. Gregory for assistance with animal care and data collection. We also thank C. Mayerl, K. Diamond, and the Clemson Writers Guild for feedback on this manuscript.

COMPETING INTERESTS

The authors declare no competing interests.

AUTHOR CONTRIBUTIONS

VKHY and RWB designed the study, collected and analyzed data, and wrote the manuscript. CW and BPW contributed to data collection and analysis and writing of the manuscript.

FUNDING

Work was supported by Clemson University Creative Inquiry Grant #479.

DATA ACCESSIBILITY

Data available from the Dryad Digital Repository: doi:10.5061/dryad.tv7fk

REFERENCES

Ashley-Ross, M. A., Hsieh, S. T., Gibb, A. C. and Blob, R. W. (2013). Vertebrate land invasions-past, present, and future: an introduction to the symposium. *Integr. Comp. Biol.* **53**, 192-196.

Bertram, J. E. A. and Biewener, A. A. (1990). Differential scaling of the long bones in the terrestrial Carnivora and other mammals. *J. Morphol.* **204**, 157-169. (doi: 10.1002/jmor.1052040205).

Biewener, A. A. and Dial, K. P. (1995). *In vivo* strain in the humerus of pigeons (*Columba livia*) during flight. *J. Morphol.* **225**, 61-75. (doi: 10.1002/jmor.1052250106).

Blob, R. W. and Biewener, A. A. (1999). *In vivo* locomotor strain in the hindlimb bones of *Alligator mississippiensis* and *Iguana iguana*: implications for the evolution of limb bone safety factor and non-sprawling limb posture. *J. Exp. Biol.* **202**, 1023-1046.

Blob, R. W., Espinoza, N. R., Butcher, M. T., Lee, A. H., D'Amico, A. R., Baig, F. and Sheffield, K. M. (2014). Diversity of limb-bone safety factors for locomotion in terrestrial vertebrates: evolution and mixed chains. *Integr. Comp. Biol.* **54**, 1058-1071.

Blob, R. W., Mayerl, C. J., Rivera, A. R. V., Rivera, G. and Young, V. K H. (2016). "On the fence" versus "all in": insights from turtles for the evolution of aquatic locomotor specializations and habitat transitions in tetrapod vertebrates. *Integr. Comp. Biol.* **56**, 1310-1322. (doi: 10.1093/icb/icw121)

Blob, R. W., Rivera, A. R. V. and Westneat, M. W. (2008). Hindlimb function in turtle locomotion: limb movements and muscular activation across taxa, environment, and ontogeny. In *Biology of Turtles*, pp. 139-162. (ed. J. Wyneken, M. H. Godfrey, V. Bels), pp. 139-162. Boca Raton, FL: CRC Press.

Buckwalter, J. A., Glimcher, M. J., Cooper, R. R. and Recker, R. (1995). Bone biology. Part I: structure, blood supply, cells, matrix, and mineralization. *J. Bone Joint Surg.* **77**, 1256 - 1275.

Butcher, M. B., Espinoza, N. R., Cirilo, S. R. and Blob, R. W. (2008). *In vivo* strains in the femur of the river cooter turtles (*Pseudemys concinna*) during terrestrial locomotion: tests of force-platform models of loading mechanics. *J. Exp. Biol*. **211,** 2397-2407. (doi: 10.1242/jeb.018986).

Caldwell, M. W. (2002). From fins to limbs to fins: limb evolution in fossil marine reptiles. *Am. J. Med. Gen*. **112**, 236-249.

Ernst, C. H. and Lovich, J. E. (2009). *Turtles of the United States and Canada*, 2nd edn. Baltimore: The Johns Hopkins University Press.

Fish, F. E. (1996). Transitions from drag-based to lift-based propulsion in mammalian swimming. *Am. Zool*. **36**, 628-641.

Gillis, G. B. and Blob, R. W. (2001). How muscles accommodate movement in different physical environments: aquatic versus terrestrial locomotion in vertebrates. *Comp. Biochem. Physiol*. **131A**, 61–75. (doi: 10.1016/S1095-6433(01)00466-4).

Lanyon, L. E., Goodship, A. E., Pye, C. and McFie, H. (1982). Mechanically adaptive bone remodeling: a quantitative study on functional adaptation in the radius following ulna osteotomy in sheep. *J. Biomech*. **12**, 141-154. (doi: 10.1016/0021-9290(82)90246-9).

Lindgren, J., Polcyn, M. J. and Young, B. A. (2011). Landlubbers to leviathans: evolution of swimming in mosasaurine mosasaurs. *Paleobiology* **37**, 445-469.

Mayerl, C. J., Brainerd, E. L. and Blob, R. W. (2016). Pelvic girdle mobility of cryptodire and pleurodire turtles during walking and swimming. *J. Exp. Biol*. **219**, 2650-2658.

Ogushi, K. (1911). Anatomische studien an der japanichen dreikralligen Lippenschildkrote (*Trionyx japonicus*). I. Das Skeletsystem. *Morpholog. Jahrbuch* **43**, 1-106.

Pace, C. M., Blob, R. W. and Westneat, M. W. (2001). Comparative kinematics of the forelimb during swimming in red-eared slider (*Trachemys scripta*) and spiny softshell (*Apalone spinifera*) turtles. *J. Exp. Biol.* **204**, 3261-3271.

Renous, S., de Lapparent de Broin, F., Depecker, M., Davenport, J. and Bels, V. (2008). Evolution of locomotion in aquatic turtles. In *Biology of Turtles*, pp. 97-133. (ed. J. Wyneken, M. H. Godfrey, V. Bels), pp. 139-162. Boca Raton, FL: CRC Press.

Rivera, A. R. V. and Blob, R. W. (2010). Forelimb kinematics and motor patterns of the slider turtle (*Trachemys scripta*) during swimming and walking: shared and novel strategies for meeting locomotor demands of water and land. *J. Exp. Biol.* **213**, 3515-3526.

Schmidt, M., Mehlhorn, M. and Fischer, M. S. (2016). Shoulder girdle rotation, forelimb movement, and the influence of carapace shape on locomotion in *Testudo hermanni* (Testudinidae). *J. Exp. Biol.* 137059. (doi: 10.1242/jeb.137059).

Sheffield, K. M., Butcher, M. T., Shugart, S. K., Gander, J. C. and Blob, R. W. (2011). Locomotor loading mechanics in the hindlimbs of tegu lizards (*Tupinambis merianae*): comparative and evolutionary implications. *J. Exp. Biol.* **214**, 2616-2630. (doi: 10.1242/jeb.048801).

Vogel, S. (2013). *Comparative Biomechanics: Life's Physical World*. Princeton, NJ: Princeton University Press.

Walker, J. A. (2002). Functional morphology and virtual models: physical constraints of the design of oscillating wings, fins, legs, and feet at intermediate Reynolds numbers. *Integr. Comp. Biol.* **42**, 232-242. (doi: 10.1093/icb/42.2.232).

Walker, W. F. Jr. (1971). A structural and functional analysis of walking in the turtle, *Chrysemys picta marginata*. *J. Morphol.* **134**, 195-214.

Wyneken, J. (1997). Sea turtle locomotion: mechanisms, behavior, and energetics. In *The Biology of Sea Turtles* (ed. P. L. Lutz and J. A. Musick), pp. 165-198. Boca Raton, FL: CRC Press.

Young, V. K H. and Blob, R. W. (2015). Limb bone loading in swimming turtles: changes in loading facilitate transitions from tubular to flipper-shaped limbs during aquatic invasions. *Biol. Lett.* **11**: 20150110. (doi: 10.1098/rsbl.2015.0110).

Young, V. K H., Vest, K. G., Rivera, A. R. V., Espinoza, N. R. and Blob, R. W. (2017). One foot out the door: limb function during swimming in terrestrial versus aquatic turtles. *Biol. Lett.* **13**: 2060732. (doi: 10,1098/rsbl.2016.0732).

Young, V. K H., Wienands, C. E., Wilburn, B. P. and Blob, R. W. (2017). Data from 'Humeral loads during swimming and walking in turtles: implications for morphological change during aquatic reinvasions'. Dryad Digital Repository. (doi: 10.5061/dryad.tv7fk).

Zimmer, C. (1999). *At the Water's Edge: Fish with Fingers, Whales with Legs, and How Life Came Ashore but then Went Back to Sea*. New York, NY: Touchstone.

Zug, G. R. (1971). Buoyancy, locomotion, morphology of the pelvic girdle and hind limb, and systematics of cryptodiran turtles. *Misc. Publ. Mus. Zool. Univ. Mich.* **142**, 1-98.

Figures

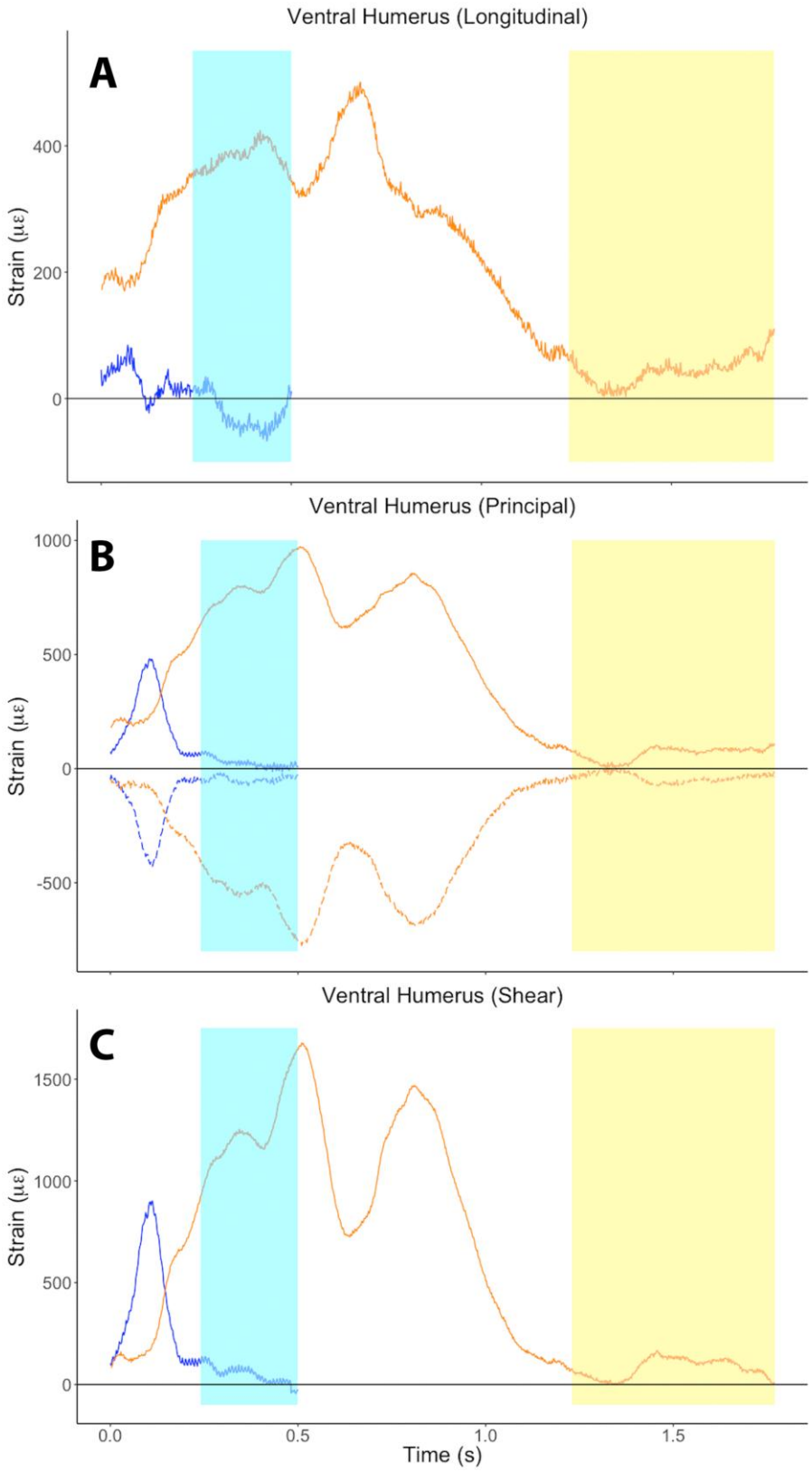

Figure 1. Examples of high magnitude strain traces from PC06, simultaneously recorded from a rosette gauge located on the ventral surface of the humerus during swimming and terrestrial walking in the river cooter turtle (*Pseudemys concinna*). A single limb cycle from the same individual is illustrated for both behaviors. (A) Ventral longitudinal strain. (B) Ventral principal strains. (C) Ventral shear strain. Walking strains are shown in orange and swimming strains are shown in blue. Shaded regions indicate the recovery (protraction) phase of the limb cycle for each locomotor behavior (walking in yellow, swimming in light blue). Compressive principal strain is represented by a dashed line. Note the duration of the swimming cycle is approximately half that of the walking cycle.

Tables

Table 1. Mann-Whitney *U* results for comparisons of peak humeral strains during thrust versus recovery phases of swimming in *P. concinna*. Values are mean ± s. e.; pT, principal tensile strain; pC, principal compressive strain; φ_T, angle of principal tensile strain to the humeral long axis.

ID	Gauge Location	Strain Type	*N*	Thrust (με)	Recovery (με)	|*Z*|	*p*
PC01	Posterior	Longitudinal	40	58.1 ± 11.9	-60.7 ± 18.8	3.30	0.0010*
PC02	Ventral	Longitudinal	71	-19.6 ± 12.6	-89.4 ± 10.6	3.22	0.0013*
	Posterior	Longitudinal	71	-13.1 ± 18.7	-88.1 ± 16.2	2.75	0.0059*
PC03	Posterior	Longitudinal	22	36.9 ± 24.2	-83.7 ± 27.5	2.27	0.0235*
PC04	Anterior	Longitudinal	34	32.7 ± 13.2	8.7 ± 12.7	1.05	0.2943
	Anterior	pT	34	72.2 ± 7.3	63.7 ± 7.4	0.98	0.3295
	Anterior	pC	34	-70.5 ± 5.8	-73.5 ± 7.0	0.35	0.7267
	Anterior	φ_T[a]	34	51.8 ± 4.1	42.9 ± 4.6	1.21	0.2270
	Anterior	Shear	34	93.8 ± 11.4	90.1 ± 13.8	0.52	0.6022
PC05	Ventral	Longitudinal	12	156.9 ± 35.6	55.2 ± 73.0	0.09	0.9310
	Ventral	pT	12	193.6 ± 26.4	155.9 ± 52.7	2.11	0.0351*
	Ventral	pC	12	-184.2 ± 32.2	-215.2 ± 49.1	0.20	0.8399
	Ventral	φ_T[a]	12	24.1 ± 7.5	48.2 ± 11.7	0.49	0.6236
	Ventral	Shear	12	137.0 ± 24.5	50.4 ± 11.0	2.68	0.0073*
PC06	Ventral	Longitudinal	85	51.6 ± 7.5	-87.3 ± 3.7	2.08	0.0376*
	Ventral	pT	85	156.2 ± 10.9	54.9 ± 6.7	8.46	<0.0001*
	Ventral	pC	85	-124.9 ± 11.5	-117.7 ± 0.1	0.22	0.8273
	Ventral	φ_T[a]	85	36.3 ± 2.0	42.6 ± 3.6	0.24	0.8104
	Ventral	Shear	85	242.4 ± 23.1	93.7 ± 16.7	6.48	<0.0001*

[a]Units for φ_T in deg.

*$p \leq 0.05$.

Table 2. Mann-Whitney *U* results for comparisons of peak humeral strains during swimming versus terrestrial walking for the thrust/stance phase of the limb cycle in *P. concinna*. Values are mean ± s. e. pT, principal tensile strain; pC, principal compressive strain; φ_T, angle of principal tensile strain to the humeral long axis.

ID	Gauge Location	Strain Type	*N* *(swim, walk)*	Swim (με)	Walk (με)	|*Z*|	*p*
PC01	Posterior	Longitudinal	40; 35	58.1 ± 11.9	1398.9 ± 37.6	7.43	<0.0001*
PC02	Ventral	Longitudinal	71; 28	-19.6 ± 12.6	251.9 ± 64.1	7.58	<0.0001*
	Posterior	Longitudinal	71; 28	-13.1 ± 18.7	277.2 ± 58.6	7.28	<0.0001*
PC03	Posterior	Longitudinal	22; 8	36.9 ± 24.2	746.4 ± 95.5	4.10	<0.0001*
PC05	Ventral	Longitudinal	12; 29	156.9 ± 35.6	562.5 ± 93.8	4.97	<0.0001*
	Ventral	pT	12; 29	193.6 ± 26.4	699.3 ± 46.1	3.97	<0.0001*
	Ventral	pC	12; 29	-184.2 ± 32.2	-249.5 ± 32.1	2.22	0.0264*
	Ventral	φ_T[a]	12; 29	24.1 ± 7.5	13.9 ± 3.7	1.42	0.1561
	Ventral	Shear	12; 29	137.0 ± 24.5	285.5 ± 30.7	2.97	0.0030*
PC06	Ventral	Longitudinal	85; 32	51.6 ± 7.5	274.2 ± 56.1	8.30	<0.0001*
	Ventral	pT	85; 32	156.2 ± 10.9	556.2 ± 31.8	7.88	<0.0001*
	Ventral	pC	85; 32	-124.9 ± 11.5	-362.2 ± 32.4	6.37	<0.0001*
	Ventral	φ_T[a]	85; 32	36.3 ± 2.0	56.7 ± 3.1	4.98	<0.0001*
	Ventral	Shear	85; 32	242.4 ± 23.1	729.2 ± 56.5	6.30	<0.0001*

[a]Units for φ_T in deg.

*$p \leq 0.05$.